Available online at www.sciencedirect.com
SCIENCE DIRECT®
ELSEVIER
Mechanism and Machine Theory 39 (2004) 905–919
Mechanism and Machine Theory
www.elsevier.com/locate/mechmt

Contact characteristics of cylindrical gears with curvilinear shaped teeth

Rui-Tang Tseng, Chung-Biau Tsay *

Department of Mechanical Engineering, National Chiao Tung University, Hsinchu 30010, Taiwan, ROC

Received 18 March 2003; received in revised form 12 February 2004; accepted 6 April 2004

Abstract

Transmission errors and bearing contacts of a curvilinear-tooth gear under different assembly conditions are investigated by applying the tooth contact analysis and the surface topology methods. Four numerical examples are presented to illustrate the influence of gear assembly errors on transmission errors and the directions and orientations of the contact ellipses. The numerical results reveal that the transmission error of the curvilinear-tooth gear pair is small and the bearing contacts are located in the middle region of the curvilinear-tooth surface even under axial misalignments.

Keywords: Curvilinear-tooth gear; Tooth contact analysis; Transmission error; Contact ellipse

1. Introduction

The spur gear set and the conventional helical gear pair with parallel axes are in line contact, and thus their transmission errors (TE) are sensitive to axial misalignments of the gear. When a gear set without tooth crowning is axially misaligned, tooth edge contact will occur and this results in stress concentration on the gear, vibration and noise. Spur and helical gears with tooth crowning can prevent edge contact induced by axial misalignments of the gear, and can also localize the bearing contacts. Litvin et al. [1,2] proposed a generation mechanism with a five-degree-of-freedom system and tooth contact analysis (TCA) for spur gear crowning to prevent gear edge contact. In this study, a curvilinear-tooth gear pair with point contacts is proposed. Gear edge contact can thus be avoided because the contact paths on gear tooth surfaces are

* Corresponding author. Tel./fax: +886-35-728-450.
E-mail address: cbtsay@mail.nctu.edu.tw (C.-B. Tsay).

0094-114X/$ - see front matter © 2004 Published by Elsevier Ltd.
doi:10.1016/j.mechmachtheory.2004.04.006

Nomenclature

a_i, b_i tool setting of rack cutter $\sum_i$ $(i = \mathrm{F, P})$
l_i variable parameter which determines the location on rack cutter $(i = \mathrm{F, P})$
r_i radius of pitch circle of gear i $(i = 1, 2)$
C' operational center distance (Fig. 1)
ΔC variation of center distance (Fig. 1)
R_i nominal radius of the face mill-cutter $(i = \mathrm{F, P})$
T_i number of teeth of gear i $(i = 1, 2)$
$X_\mathrm{T}^{(i)}, Y_\mathrm{T}^{(i)}, Z_\mathrm{T}^{(i)}$ coordinates of gear tooth surface i $(i = 1, 2)$ represented in coordinate system S_T (Fig. 2)
$\mathbf{n}_\mathrm{c}^{(i)}$ unit normal vector of surface $\sum_i$ $(i = \mathrm{F, P})$ represented in coordinate system S_c
$\mathbf{R}_\mathrm{c}^{(i)}$ position vector of surface $\sum_i$ $(i = \mathrm{F, P})$ represented in coordinate system S_c
(r, θ) auxiliary polar coordinate system represented on contact tooth tangent plane (Fig. 2)
$S_i(X_i, Y_i, Z_i)$ coordinate system i $(i = 1, 2, \mathrm{v, h, f, T})$ with three orthogonal axes X_i, Y_i, and Z_i
$\Delta\gamma_\mathrm{h}$ horizontal axial misalignment (in degrees, Fig. 1)
$\Delta\gamma_\mathrm{v}$ vertical axial misalignment (in degrees, Fig. 1)
θ_i variable parameter which determines the location on rack cutter $(i = \mathrm{F, P})$
ϕ_i rotation angle of gear i $(i = 1, 2)$ when gear i is generated by rack cutter
ϕ'_i rotation angle of gear i $(i = 1, 2)$ when two gears mesh with each other (Fig. 1)
$\Delta\phi'_2(\phi'_1)$ transmission errors (in arc-second)
$\psi_\mathrm{n}^{(i)}$ normal pressure angle of rack cutter $\sum_i$ $(i = \mathrm{F, P})$

Subscripts
F, P rack cutter surface to generate tooth surfaces of pinion and gear
1, 2 tooth surfaces of pinion and gear

located near the middle region of the tooth flank even when the gear set is meshed with axial misalignments.

The transmission error (TE) of a mating gear pair is an important factor for gear noise and vibration criteria. Litvin and Tsay [3] simulated the meshing and bearing contact of circular arc helical gears. Litvin [4,5] and Tsay [6] investigated the TCA of some other types of meshing gear pairs under different meshing conditions. Lin et al. [7] performed TCA for hypoid gears. Chang et al. [8] analyzed the kinematic optimization of a modified helical gear train. Litvin et al. [9,10] proposed a surface synthesis method by utilizing a predesigned parabolic transmission errors function to absorb the transmission errors of an approximately linear function of the designed gear pair induced by axial misalignments of the gear. Zhang and Fang [11] considered the elastic deformation of tooth surfaces to estimate the transmission errors of helical gears under a load. Umeyama et al. [12] investigated the loaded transmission errors of helical gears and the relationship between the actual contact ratio and effective contact ratio. Since the contact type of the curvilinear-tooth gear proposed herein is a point contact, the transmission error of the gear pair is not sensitive to the axial misalignments of the gear and the transmission error is small.

When two gear tooth surfaces are meshed, the instantaneous contact point of the two surfaces is spread over an elliptical area due to elasticity of the tooth surface under load. Litvin [4,5] applied principal directions and principal curvatures to estimate the orientations and dimensions of contact ellipses on the common tangent plane of the two mating tooth surfaces. Janninck [13] proposed a contact surface topology method to predict the initial contact pattern on worm and worm gear drives.

The TCA technology has been utilized herein to investigate the transmission errors of the curvilinear-tooth gear pair under ideal and error assembly conditions. The contact ellipses of the curvilinear-tooth gears can be obtained by applying the contact surface topology method. The results reveal that the nominal radius of the face mill-cutter is the important design parameter which influences the dimensions of gear contact ellipses.

2. Mathematical model of the curvilinear-tooth gears

The mathematical model of cylindrical gears with curvilinear shaped teeth adopted herein was developed in our previous study [15]. In this paper, only the mathematical models of the active tooth surfaces of the pinion and the gear are expressed and discussed. The profile of the rack cutter's normal middle section is the same as that for the straight-edge rack cutter that generates the tooth profile of involute gears. The right-side of the rack cutter surface $\sum_{FR}$ is used to produce the left-side of the curvilinear pinion tooth surface $\sum_{1L}$, while the left-side of the rack cutter surface $\sum_{FL}$ is used to generate the right-side of the curvilinear pinion tooth surface $\sum_{1R}$. The gear and pinion with curvilinear shaped teeth proposed in this investigation are produced by the same face mill-cutter [14]. The rack cutter with a circular-arc tooth profile is considered as the generating tool for the gear generation.

The equation of the circular-arc imaginary rack cutter surface $\sum_{FR}$ and its unit normal vector can be expressed as [15]

$$\mathbf{R}_c^{(F)} = \begin{bmatrix} l_F \cos\psi_n^{(F)} - a_F \\ (l_F \sin\psi_n^{(F)} + b_F - a_F \tan\psi_n^{(F)})\cos\theta_F + R_F(1-\cos\theta_F) \\ -(l_F \sin\psi_n^{(F)} + b_F - a_F \tan\psi_n^{(F)})\sin\theta_F + R_F\sin\theta_F \end{bmatrix} \tag{1}$$

and

$$\mathbf{n}_c^{(F)} = \begin{bmatrix} \sin\psi_n^{(F)} \\ -\cos\psi_n^{(F)}\cos\theta_F \\ \cos\psi_n^{(F)}\sin\theta_F \end{bmatrix}, \tag{2}$$

where parameters a_F, b_F, $\psi_n^{(F)}$ and R_F are the design parameters of the rack cutter, and l_F and θ_F are surface coordinates of the rack cutter.

According to the generation mechanism described in a previous study [15], the generated pinion tooth surface can be obtained as follows:

$$f_1(l_F,\theta_F,\phi_1) = [l_F - a_F(\cos\psi_n^{(F)} + \tan\psi_n^{(F)}\sin\psi_n^{(F)}) + b_F\sin\psi_n^{(F)}]\cos\theta_F + (R_F(1-\cos\theta_F) - r_1\phi_1)\sin\psi_n^{(F)} = 0, \tag{3}$$

$$\mathbf{R}_1^{(F)} = \begin{bmatrix} \cos\phi_1 & -\sin\phi_1 & 0 & r_1(\cos\phi_1 + \phi_1\sin\phi_1) \\ \sin\phi_1 & \cos\phi_1 & 0 & r_1(\sin\phi_1 - \phi_1\cos\phi_1) \\ 0 & 0 & 1 & 0 \\ 0 & 0 & 0 & 1 \end{bmatrix} \mathbf{R}_c^{(F)}. \tag{4}$$

The unit normal vector of the generated pinion tooth surface can also be obtained by

$$\mathbf{n}_1^{(F)} = \begin{bmatrix} \cos\phi_1\sin\psi_n^{(F)} + \sin\phi_1\cos\psi_n^{(F)}\cos\theta_F \\ \sin\phi_1\sin\psi_n^{(F)} - \cos\phi_1\cos\psi_n^{(F)}\cos\theta_F \\ \cos\psi_n^{(F)}\sin\theta_F \end{bmatrix}. \tag{5}$$

Eq. (3) is termed the equation of meshing and Eq. (4) represents the locus of the rack cutter surfaces. The mathematical model of the left-side curvilinear pinion tooth surface $\sum_{1L}$ can be obtained by considering Eqs. (3) and (4), simultaneously. Similarly, the gear tooth surfaces can be generated by using the same rack cuter or another rack cutter, e.g. $\sum_{P}$. The circular-arc imaginary rack cutter surface $\sum_{PL}$ used to produce the right-side curvilinear-tooth gears and its unit normal vector are expressed as

$$\mathbf{R}_c^{(P)} = \begin{bmatrix} -l_P\cos\psi_n^{(P)} + a_P \\ -(l_P\sin\psi_n^{(P)} + b_P - a_P\tan\psi_n^{(P)})\cos\theta_P + R_P(1-\cos\theta_P) \\ (l_P\sin\psi_n^{(P)} + b_P - a_P\tan\psi_n^{(P)})\sin\theta_P + R_P\sin\theta_P \end{bmatrix} \tag{6}$$

and

$$\mathbf{n}_c^{(P)} = \begin{bmatrix} -\sin\psi_n^{(P)} \\ \cos\psi_n^{(P)}\cos\theta_P \\ -\cos\psi_n^{(P)}\sin\theta_P \end{bmatrix}. \tag{7}$$

Therefore, the mathematical model of the right-side of the curvilinear gear tooth surface $\sum_{2R}$ can also be developed by the same process and represented as follows:

$$f_2(l_P,\theta_P,\phi_2) = -[l_P - a_P(\cos\psi_n^{(P)} + \tan\psi_n^{(P)}\sin\psi_n^{(P)}) + b_P\sin\psi_n^{(P)}]\cos\theta_P + (R_P(1-\cos\theta_P) - r_2\phi_2)\sin\psi_n^{(P)} = 0, \tag{8}$$

$$\mathbf{R}_2^{(P)} = \begin{bmatrix} \cos\phi_2 & \sin\phi_2 & 0 & -r_2(\cos\phi_2 + \phi_2\sin\phi_2) \\ -\sin\phi_2 & \cos\phi_2 & 0 & r_2(\sin\phi_2 - \phi_2\cos\phi_2) \\ 0 & 0 & 1 & 0 \\ 0 & 0 & 0 & 1 \end{bmatrix} \mathbf{R}_c^{(P)}. \tag{9}$$

The unit normal vector of the generated gear tooth surface can be obtained by

$$\mathbf{n}_2^{(P)} = \begin{bmatrix} -\cos\phi_2\sin\psi_n^{(P)} + \sin\phi_2\cos\psi_n^{(P)}\cos\theta_P \\ \sin\phi_2\sin\psi_n^{(P)} + \cos\phi_2\cos\psi_n^{(P)}\cos\theta_P \\ -\cos\psi_n^{(P)}\sin\theta_P \end{bmatrix}. \tag{10}$$

Substituting Eq. (8) into Eq. (9) yields the mathematical model of the right-side curvilinear gear tooth surface $\sum_{2R}$, and Eq. (10) expresses its unit normal vector represented in coordinate system $S_2(X_2, Y_2, Z_2)$.

3. Simulation of gear meshing and tooth contact analysis

The model for gear meshing with assembly errors can be simulated by changing the settings and orientations of the coordinate systems $S_h(X_h, Y_h, Z_h)$ and $S_v(X_v, Y_v, Z_v)$ with respect to the fixed coordinate system $S_f(X_f, Y_f, Z_f)$ as shown in Fig. 1, where coordinate systems $S_1(X_1, Y_1, Z_1)$ and $S_2(X_2, Y_2, Z_2)$ are attached to the pinion and gear, respectively. The axes Z_1 and Z_2 are rotational axes of the pinion and gear, respectively. Coordinate systems $S_v(X_v, Y_v, Z_v)$ and $S_h(X_h, Y_h, Z_h)$ are the reference coordinate systems for the misaligned gear assembly simulations. The simulation of horizontal axial misalignment of the gear may be achieved by rotating the coordinate system $S_h(X_h, Y_h, Z_h)$ about the X_h axis through an angle $\Delta\gamma_h$ with respect to the coordinate system $S_f(X_f, Y_f, Z_f)$. Similarly, simulation of vertical axial misalignment of the gear can be performed by rotating the coordinate system $S_v(X_v, Y_v, Z_v)$ about the Y_h axis through an angle $\Delta\gamma_v$ with respect to coordinate system $S_h(X_h, Y_h, Z_h)$. Symbol C' represents the operational center distance of the gear pair rotational axes, and ΔC denotes the center distance variation. The origin O_2 of the coordinate system $S_2(X_2, Y_2, Z_2)$ may be displaced by an amount of ΔC and the operational center distance of the meshing gear pair can be represented by $C' = C + \Delta C$ with respect to origin O_f of the fixed coordinate system $S_f(X_f, Y_f, Z_f)$. ϕ_1' and ϕ_2' represent the rotational angles of the pinion and gear, respectively, when they are meshed with each other. When applying the tooth contact analysis method to calculate the transmission errors of the curvilinear gear pair, the unit normal and

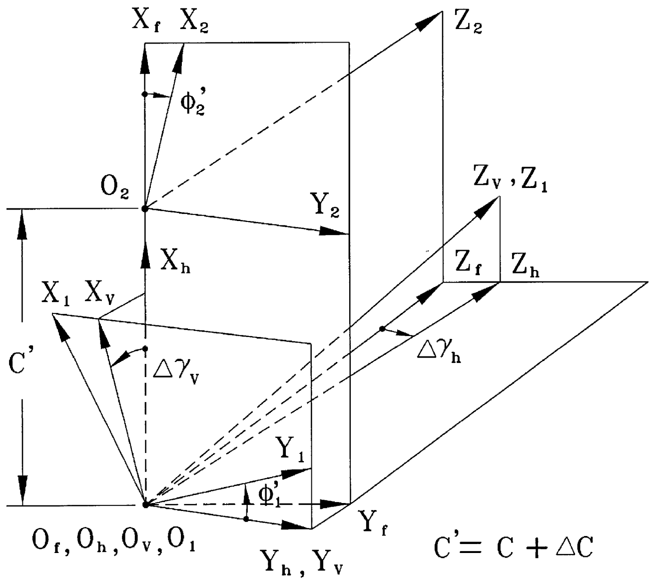

Fig. 1. Simulation of gear meshing with assembly errors.

position vectors of both pinion and gear tooth surfaces should be represented in the same coordinate system, say $S_f(X_f, Y_f, Z_f)$.

Owing to the tangency of two contacting gear tooth surfaces, the position vectors of the pinion and gear tooth surfaces should be the same at the contact point and their unit normal vectors should be collinear to each other. Therefore, the following equations must hold [4,5]:

$$\mathbf{R}_f^{(1)} - \mathbf{R}_f^{(2)} = 0 \tag{11}$$

and

$$\mathbf{n}_f^{(1)} \times \mathbf{n}_f^{(2)} = 0, \tag{12}$$

where $\mathbf{R}_f^{(1)}$ and $\mathbf{R}_f^{(2)}$ indicate the position vectors of the tooth surfaces of pinion and gear, respectively, represented in coordinate system $S_f(X_f, Y_f, Z_f)$. $\mathbf{n}_f^{(1)}$ and $\mathbf{n}_f^{(2)}$ express the surface unit normal vectors of pinion and gear, respectively, represented in coordinate system $S_f(X_f, Y_f, Z_f)$. Eq. (11) indicates that the pinion and gear tooth surfaces have a common contact point, and Eq. (12) indicates that the unit normal vectors of the pinion and gear surfaces are collinear at their contact point. Since $|\mathbf{n}_f^{(1)}| = |\mathbf{n}_f^{(2)}| = 1$, Eqs. (11) and (12) yield a system of five independent equations with six unknowns: l_F, θ_F, l_P, θ_P, ϕ_1' and ϕ_2', where l_F and θ_F are tooth surface parameters of the pinion while l_P and θ_P are tooth surface parameters of gear. If the pinion is a driving gear, the rotation angle ϕ_1' is considered a known parameter (i.e. a given value). Therefore, five unknown parameters are solved with five nonlinear equations.

The transmission errors of the curvilinear gear pair can be calculated by using the following equation:

$$\Delta\phi_2'(\phi_1') = \phi_2'(\phi_1') - \frac{T_1}{T_2}\phi_1', \tag{13}$$

where T_1 and T_2 denote the tooth numbers of pinion and gear, respectively. $\phi_2'(\phi_1')$, which represents the actual rotational angle of the gear pair meshing under different assembly conditions, is solved by numerical method. $\Delta\phi_2'(\phi_1')$ expresses the transmission error of the curvilinear gear pair under the given assembly errors.

4. Contact ellipses

When tooth surfaces are meshed with each other, their instantaneous contact point is spread over an elliptical area owing to elastic deformation. Fig. 2(a) shows that two mating surfaces $\sum_1$ and $\sum_2$ are tangential to each other at the instantaneous contact point O_T, where **n** represents the common unit normal vector at contact point O_T, which can be determined by the TCA computer simulation program. Plane T denotes the common tangent plane of the two mating surfaces. The origin of coordinate system $S_T(X_T, Y_T, Z_T)$ and the instantaneous contact point O_T are coincident. The direction of axis Z_T is defined to coincide with the common unit normal vector **n**. Thus, the plane X_T–Y_T is the common tangent plane.

In this study, the contact ellipses of the gear pair are obtained by using the surface separation topology method. To calculate the separation distance of two mating tooth surfaces, surface coordinates of the mating curvilinear-tooth gear and pinion must be transformed to the same

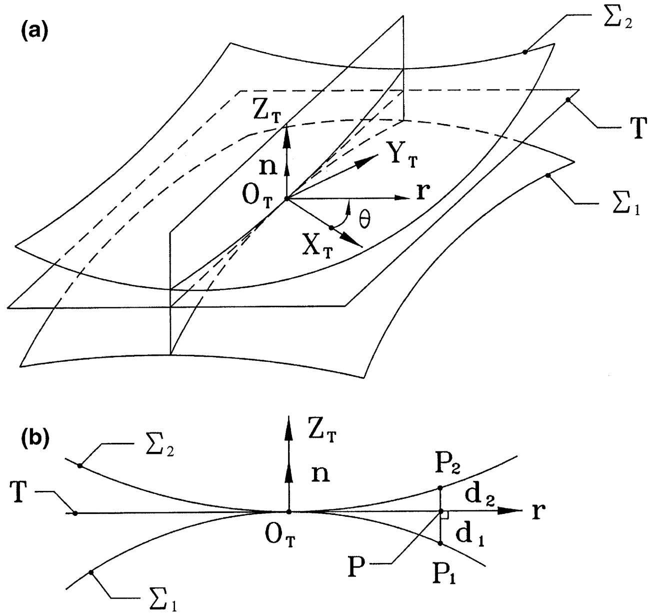

Fig. 2. (a) Common tangent plane and polar coordinates. (b) Measurements on surface separation.

coordinate system $S_T(X_T, Y_T, Z_T)$. Fig. 2(b) shows the separation distances between the surfaces $\sum_1$ and $\sum_2$ at point P of the tangent plane T. The separation distance of two mating surfaces can be defined by $d_1 + d_2$, where $d_1 + d_2$ is equal to $|Z_T^{(1)} - Z_T^{(2)}|$, measured from any point P on the tangent plane T along its perpendicular direction. $Z_T^{(1)}$ and $Z_T^{(2)}$ represent the coordinates of the Z_T component of points P_1 and P_2, respectively. The equal distance-separation line for two mating surfaces, which is found by defining an auxiliary polar coordinate system (r, θ), can be represented by the following system of nonlinear equations:

$$X_T^{(1)} = X_T^{(2)}, \tag{14}$$

$$Y_T^{(1)} = Y_T^{(2)} \tag{15}$$

$$\tan(\theta) = \frac{Y_T^{(1)}}{X_T^{(1)}} \tag{16}$$

and

$$|Z_T^{(1)} - Z_T^{(2)}| = 0.00632 \text{ mm}, \tag{17}$$

where $X_T^{(1)}$, $Y_T^{(1)}$, $X_T^{(2)}$ and $Y_T^{(2)}$ are coordinates of points P_1 and P_2 on the tangent plane X_T–Y_T, respectively. Eqs. (14)–(17) consist of a system of four independent nonlinear equations with five unknowns: l_F, θ_F, l_P, θ_P and θ. Here l_F and θ_F are tooth surface parameters of the pinion while l_P and θ_P denote tooth surface parameters of the gear. Parameter θ represents the angle measured from axis X_T to axis r on the common tangent plane T. The thickness of the coating paint used for contact pattern tests is 0.00632 mm. Parameter θ can be considered a known parameter with a range of $-\pi$ to π. Therefore, the four unknown parameters are solved with four equations by a numerical method. Thus, the dimension and shape of contact ellipses can be found.

5. Numerical examples for gear meshing simulations

Example 1. The gear parameters are given as follows: teeth numbers $T_1 = 18$, $T_2 = 36$, normal pressure angles $\psi_n^{(F)} = \psi_n^{(P)} = 20°$, normal module $M_n = 3$ mm, face width = 30 mm, nominal radius of face mill-cutter $R_i = 30$ mm ($i = \mathrm{F, P}$). If two mating gears are meshing under ideal conditions, it means that the misaligned angles $\Delta\gamma_h = \Delta\gamma_v = 0.0°$, and $\Delta C = 0.0$ mm. The bearing contacts and transmission errors for ideal meshing condition are shown in Table 1. Table 1 demonstrates that the curvilinear-tooth gear pair does not induce transmission errors under ideal condition. The parameters $\theta_F = \theta_P = 0.0°$ shown in Table 1 indicates that the contact points are distributed over the middle region of the tooth flank when the gear pair is meshed under ideal assembly conditions. Fig. 3 depicts the contact path and the contact ellipses on the pinion tooth surface under ideal assembly conditions. The contact ellipses are plotted when the pinion is rotated every 4° form −6° to 18°. Three different values of the nominal radius of the face mill-cutter R_i, namely 30, 50 and 100 mm, were chosen to demonstrate the effects of R_i on the corresponding contact ellipses. Fig. 3 also reveals that the length of the major axis of the contact ellipses is proportional to the radius of the face mill-cutter R_i. Fig. 4 shows the relationship between the radius of face mill-cutter R_i and the ratio of the major and minor axes of the contact ellipse a/b is in linear. When the radius of a face mill-cutter is 30, 50 and 100 mm, respectively, the ratio a/b is 6.14, 9.93 and 19.39, as shown in Fig. 4.

Example 2. Table 2 lists the analysis results of bearing contacts and transmission errors using the same gear design parameters as those given in Example 1 with $\Delta\gamma_h = \Delta\gamma_v = 0.0°$, and $\Delta C = 0.5$ mm (0.62%). The contact points of the curvilinear-tooth gear pair are dislocated but the mating gear pair does not induce transmission errors at all under center distance variation. Table 2 illustrates that the contact points are still distributed over the middle region of the tooth flank.

Table 1
Transmission errors and bearing contacts for ideal meshing condition

ϕ_1' (deg)	ϕ_2' (deg)	θ_F (deg)	θ_P (deg)	l_F (mm)	l_P (mm)	TE (arc-sec.)
−10.00	−5.00	0.000	0.000	0.774	5.610	0.000
−8.00	−4.00	0.000	0.000	1.097	5.287	0.000
−6.00	−3.00	0.000	0.000	1.419	4.965	0.000
−4.00	−2.00	0.000	0.000	1.741	4.643	0.000
−2.00	−1.00	0.000	0.000	2.064	4.320	0.000
0.00	0.00	0.000	0.000	2.386	3.998	0.000
2.00	1.00	0.000	0.000	2.709	3.676	0.000
4.00	2.00	0.000	0.000	3.031	3.353	0.000
6.00	3.00	0.000	0.000	3.353	3.031	0.000
8.00	4.00	0.000	0.000	3.676	2.709	0.000
10.00	5.00	0.000	0.000	3.998	2.386	0.000

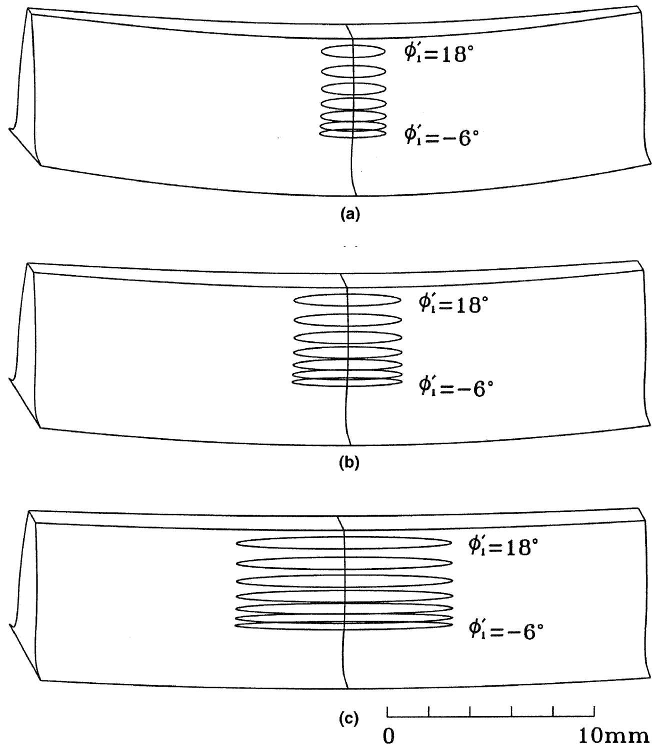

Fig. 3. Contact path and contact ellipses on the pinion tooth surface under ideal assembly condition.

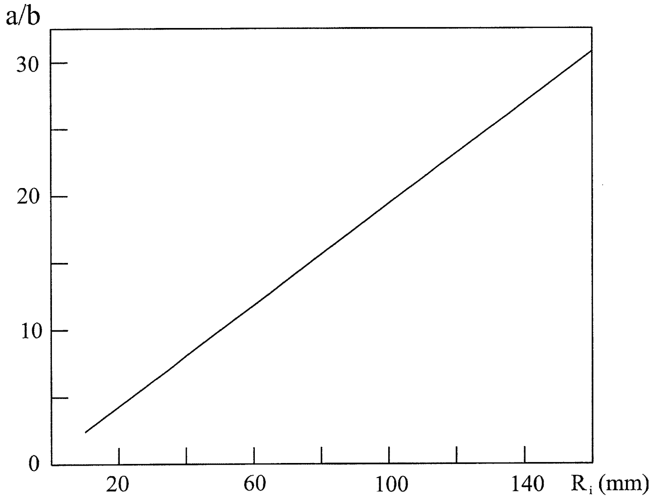

Fig. 4. Relationship between the ratio a/b and nominal radius of face mill-cuter R_i.

The contact characteristic of the curvilinear-tooth gears is similar to that of spur gears when two spur gears are meshing with center distance variation.

Table 2
Transmission errors and bearing contacts due to center distance variation $\Delta C = 0.5$ mm

ϕ_1' (deg)	ϕ_2' (deg)	θ_F (deg)	θ_P (deg)	l_F (mm)	l_P (mm)	TE (arc-sec.)
−10.00	−5.00	0.000	0.000	0.927	5.978	0.000
−8.00	−4.00	0.000	0.000	1.249	5.655	0.000
−6.00	−3.00	0.000	0.000	1.571	5.333	0.000
−4.00	−2.00	0.000	0.000	1.894	5.011	0.000
−2.00	−1.00	0.000	0.000	2.216	4.688	0.000
0.00	0.00	0.000	0.000	2.538	4.366	0.000
2.00	1.00	0.000	0.000	2.861	4.044	0.000
4.00	2.00	0.000	0.000	3.183	3.721	0.000
6.00	3.00	0.000	0.000	3.505	3.399	0.000
8.00	4.00	0.000	0.000	3.828	3.077	0.000
10.00	5.00	0.000	0.000	4.150	2.754	0.000

Example 3. The horizontal axial misalignment of the gear $\Delta\gamma_h = 0.1°$ is considered when two mating curvilinear-tooth gears are meshed. The gear design parameters are the same as those given in Example 1. The bearing contacts and transmission errors of the gear pair under the prescribed horizontal axial misalignment are given in Table 3. In this case the contact points are distributed near the middle section of the tooth flank so that the edge contact will not occur. Since the contact type of the curvilinear-tooth gear pair proposed here is a point contact, the transmission errors of this type of gear pairs are not sensitive to axial misalignments of the gear.

When the curvilinear-tooth gear pair is meshed with horizontal axial misalignments $\Delta\gamma_h = 0.1°$ and $\Delta\gamma_h = -0.1°$, the bearing contacts and contact ellipses are depicted in Fig. 5(a) and (b), respectively. It is found that the bearing contacts are localized near the middle region of the tooth flank.

Example 4. The gear design parameters are chosen the same as those in Example 1. The gear pair with vertical axial misalignment $\Delta\gamma_v = 0.1°$ is considered when two mating curvilinear-tooth gears are meshed. The bearing contacts and transmission errors of the gear pair under the prescribed

Table 3
Transmission errors and bearing contacts due to horizontal axial misalignment $\Delta\gamma_h = 0.1°$

ϕ_1' (deg)	ϕ_2' (deg)	θ_F (deg)	θ_P (deg)	l_F (mm)	l_P (mm)	TE (arc-sec.)
−10.00	−4.99989	−0.836	−0.736	0.773	5.611	0.403
−8.00	−3.99991	−0.816	−0.716	1.096	5.288	0.318
−6.00	−2.99993	−0.796	−0.696	1.418	4.966	0.235
−4.00	−1.99996	−0.776	−0.676	1.741	4.644	0.154
−2.00	−0.99998	−0.756	−0.656	2.063	4.321	0.076
0.00	0.00000	−0.736	−0.636	2.385	3.999	0.000
2.00	0.99998	−0.716	−0.616	2.708	3.676	−0.074
4.00	1.99996	−0.696	−0.596	3.030	3.354	−0.146
6.00	2.99994	−0.676	−0.576	3.353	3.031	−0.216
8.00	3.99992	−0.656	−0.556	3.675	2.709	−0.283
10.00	4.99990	−0.636	−0.536	3.997	2.387	−0.349

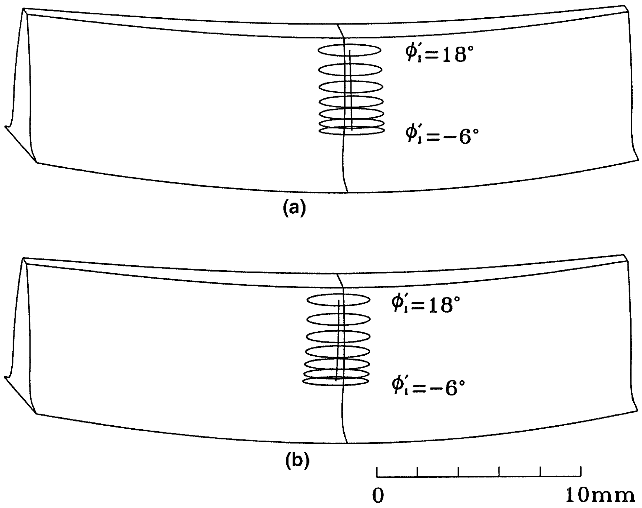

Fig. 5. Contact path and contact ellipses on the pinion tooth surface under horizontal axial misalignments.

vertical axial misalignment are listed in Table 4. In this case the contact points are also distributed near the middle section of the tooth flank. Since the curvilinear-tooth gear pair proposed here is in point contact, the transmission error of the gear pair is not sensitive to axial misalignments of the gear. The transmission errors of the curvilinear-tooth gears induced by horizontal axial misalignments are larger than those induced by vertical axial misalignments.

Fig. 6 illustrates the bearing contacts and contact ellipses of the curvilinear-tooth gear pair on pinion tooth surfaces under vertical axial misalignments $\Delta\gamma_v = +0.1°$ and $\Delta\gamma_v = -0.1°$, respectively. It is found that the bearing contacts are also localized near the middle region of the tooth flank.

The design parameters of the helical gear, such as tooth number, normal pressure angle, normal module and face width, are the same as those given in Example 1 and helix angle is 15°. Table 5 illustrates the bearing contacts and transmission errors of the helical gear pair meshed under

Table 4
Transmission errors and bearing contacts due to vertical axial misalignment $\Delta\gamma_v = 0.1°$

ϕ_1' (deg)	ϕ_2' (deg)	θ_F (deg)	θ_P (deg)	l_F (mm)	l_P (mm)	TE (arc-sec.)
−10.00	−5.00002	−0.268	−0.304	0.774	5.610	−0.060
−8.00	−4.00001	−0.275	−0.312	1.097	5.288	−0.049
−6.00	−3.00001	−0.282	−0.319	1.419	4.965	−0.037
−4.00	−2.00001	−0.290	−0.326	1.741	4.643	−0.025
−2.00	−1.00000	−0.297	−0.333	2.064	4.321	−0.012
0.00	0.00000	−0.304	−0.341	2.386	3.998	0.000
2.00	1.00000	−0.312	−0.348	2.709	3.676	0.013
4.00	2.00001	−0.319	−0.355	3.031	3.354	0.026
6.00	3.00001	−0.326	−0.363	3.353	3.031	0.039
8.00	4.00001	−0.333	−0.370	3.676	2.709	0.053
10.00	5.00002	−0.341	−0.377	3.998	2.386	0.068

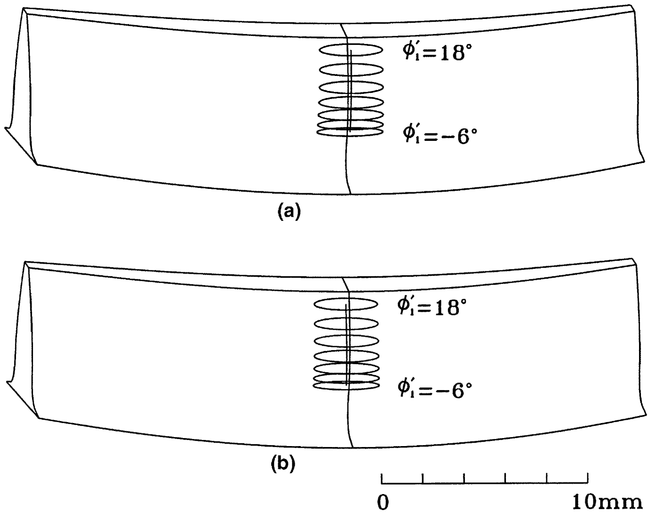

Fig. 6. Contact path and contact ellipses on the pinion tooth surface under vertical axial misalignments.

Table 5
Transmission errors and bearing contact due to vertical axial misalignment $\Delta\gamma_v = 0.1°$ for the helical gear pair

ϕ_1' (deg)	ϕ_2' (deg)	Z_1 (mm)	Z_2 (mm)	l_F (mm)	l_P (mm)	TE (arc-sec.)
−10.000	−4.99923	−14.95263	−15.000	2.328	4.055	2.773
−8.000	−3.99938	−14.95207	−15.000	2.671	3.713	2.218
−6.000	−2.99954	−14.95151	−15.000	3.013	3.370	1.663
−4.000	−1.99969	−14.95094	−15.000	3.356	3.028	1.109
−2.000	−0.99985	−14.95038	−15.000	3.699	2.686	0.554
0.000	0.00000	−14.94982	−15.000	4.041	2.343	0.000
2.000	0.99985	−14.94926	−15.000	4.384	2.001	−0.554
4.000	1.99969	−14.94870	−15.000	4.727	1.659	−1.109
6.000	2.99954	−14.94814	−15.000	5.070	1.317	−1.664
8.000	3.99938	−14.94757	−15.000	5.412	0.974	−2.218
10.000	4.99923	−14.94701	−15.000	5.755	0.632	−2.773

vertical axial misalignment $\Delta\gamma_v = 0.1°$. The Z_1 and Z_2 coordinates shown in Table 5 represent the location of contact points on tooth surfaces. It is found that on the edge of gear tooth surface, say $Z_2 = -15$ mm, and the tooth surface of pinion are in continuous tangency under vertical axial misalignments. Furthermore, the transmission errors of the helical gear are larger than that of the curvilinear-tooth gear with the same meshing condition of axial misalignments.

The gear design parameters are also chosen the same as those of in Example 1. When two mating gears are meshed under $\Delta\gamma_h = 0.1°$, $\Delta\gamma_h = 0.15°$, $\Delta\gamma_v = 0.15°$, $\Delta\gamma_v = 0.3°$, and $\Delta C = \pm 0.5$ mm, respectively, the relationship between the nominal radius of the face mill-cutter and transmission errors of the curvilinear-tooth gear is shown in Fig. 7(a). Line A denotes that the mating gear pair does not induce transmission errors under center distance variations. It is found that a larger R_i results in a larger TE of the gear pair under the same axial misalignment. When the

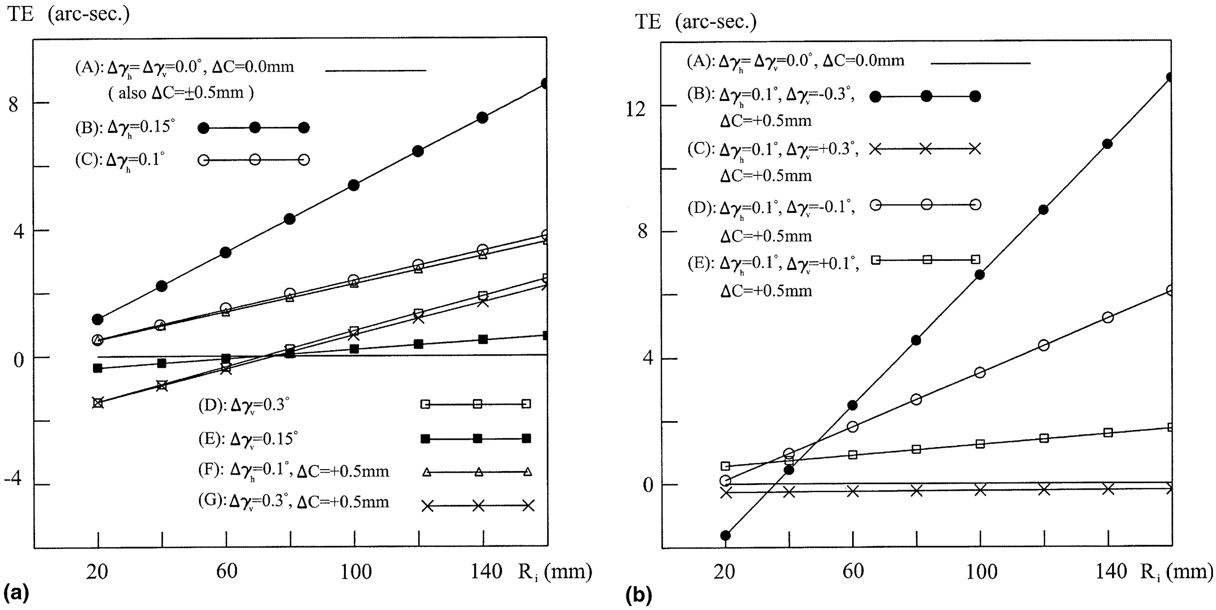

Fig. 7. (a) and (b) Relationship of transmission errors and nominal radius of the face mill-cutter R_i under different assembly conditions.

curvilinear-tooth gears generated by the radius of face mill-cutter $R_i = 71.82$ mm are meshed with vertical axial misalignments, the transmission error of the gear pair approaches to zero. Fig. 7(b) indicates that different assembly conditions result in different relationship of R_i and TE. Line B indicates that the gear pair with the radius of face mill-cutter $R_i = 35.72$ mm receives a zero TE under assembly condition B. The ratio of major and minor axes of the contact ellipse, a/b, as shown in Fig. 4 is 7.2 when the radius of face mill-cutter is 35.72 mm.

According to Fig. 4, if choosing the ratio a/b less than 10, then the largest radius of face mill-cutter becomes 50.38 mm. When the assembly condition of the gear pair is the same as that of Fig. 7(b) and choosing R_i less than 60 mm, the TE of the gear pair is less than $4''$. Owning to the limit of a face mill-cutter to generate curvilinear-tooth gears, it is clear that the diameter of the face mill-cutter must be larger than the tooth face width. Therefore, R_i must be greater than half of the tooth face width.

6. Conclusions

Based on the mathematical model of curvilinear-tooth gears, the transmission errors and bearing contacts of the gear set were investigated by using the TCA computer simulation programs. The contact ellipses of the curvilinear-tooth gear pair under different assembly conditions can be estimated by utilizing the surface topology method. According to the numerical results, the following conclusions can be drawn:

(1) The bearing contacts are localized in the middle region of the tooth flank and no transmission errors are induced when a gear pair is meshed under ideal assembly condition.
(2) The curvilinear-tooth gear pair will not induce transmission errors while the gear pair is meshed with center distance variations.
(3) Since the curvilinear-tooth gear proposed in this paper is in point contact, the gear set is not sensitive to axial misalignments of the gear, and the transmission errors are small when the gear pair is meshed under error assembly conditions. Tooth edge contact can be avoided because the contact paths are located near the middle region of the tooth flank.
(4) When the curvilinear-tooth gear pair is meshed under a non-ideal operating condition, for example under axial misalignments or variations of center distances, the dimension of the contact ellipses is almost the same as that of the gear pair meshing under ideal assembly conditions.
(5) The most important design parameter which influences the dimensions of gear contact ellipses is the nominal radius of face mill-cutter. The length of the major axis of the contact ellipses is directly proportional to the radius of face mill-cutter.

Acknowledgements

The authors are grateful to the National Science Council of the ROC for the grant. Part of this work was performed under contract No. NSC 91-2212-E-009-031.

References

[1] F.L. Litvin, J. Zhang, R.F. Handschuh, Crowned spur gears: methods for generation and tooth contact analysis—Part 1: Basic concepts, generation of the pinion tooth surface by a surface by a plane, ASME Journal of Mechanisms, Transmissions and Automation in Design 110 (1988) 337–342.
[2] F.L. Litvin, J. Zhang, R.F. Handschuh, Crowned spur gears: methods for generation and tooth contact analysis—Part 2: Generation of the pinion tooth surface by a surface of revolution, ASME Journal of Mechanisms, Transmissions and Automation in Design 110 (1988) 343–347.
[3] F.L. Litvin, C.B. Tsay, Helical gears with circular arc teeth: simulation of conditions of meshing and bearing contact, ASME Journal of Mechanisms, Transmission, and Automation in Design 107 (1985) 556–564.
[4] F.L. Litvin, Theory of Gearing, NASA Reference Publication 1212, Washington, DC, 1989.
[5] F.L. Litvin, Gear Geometry and Applied Theory, PTR Prentice Hall, Englewood Cliffs, NJ, 1994.
[6] C.B. Tsay, Helical gears with involute shaped teeth: geometry, computer simulation, tooth contact analysis, and stress analysis, ASME Journal of Mechanisms, Transmissions and Automation in Design 110 (1988) 482–491.
[7] C.Y. Lin, C.B. Tsay, Z.H. Fong, Tooth contact analysis of hypoid gears, Journal of the Chinese Society of Mechanical Engineers 17 (3) (1996) 241–249.
[8] S.L. Chang, C.B. Tsay, C.H. Tseng, Kinematic optimization of a modified helical gear train, ASME Journal of Mechanical Design 119 (2) (1997) 307–314.
[9] F.L. Litvin, J. Zhang, R.F. Handschuh, J.J. Coy, Topology of modified helical gears, Surface Topography (March) (1989) 41–58.
[10] F.L. Litvin, N.X. Chen, C.L. Hsiao, R.F. Handschuh, Generation of helical gears with new surfaces topology by application of CNC machines, Gear Technology (January/February) (1994) 30–33.
[11] Y. Zhang, Z. Fang, Analysis of transmission errors under load of helical gears with modified tooth gears, ASME Journal of Mechanical Design 119 (1997) 120–126.

[12] M. Umeyama, M. Kato, K. Inoue, Effects of gear dimensions and tooth surface modifications on the loaded transmission error of a helical gear pair, ASME Journal of Mechanical Design 120 (1998) 119–125.
[13] W.K. Janninck, Contact surface topology of worm gear teeth, Gear Technology (March/April) (1988) 31–47.
[14] S.T. Liu, Curvilinear cylindrical gears, Gear Technology (May/June) (1988) 8–12.
[15] R.T. Tseng, C.B. Tsay, Mathematical model and undercutting of cylindrical gears with curvilinear shaped teeth, Mechanism and Machine Theory 36 (2001) 1189–1202.